7-25-2013

Ptpn11 Deletion in A Novel Cartilage Cell Causes Metachondromatosis by Activating Hedgehog Signaling

Qian Wu
University of Connecticut School of Medicine and Dentistry

Published in final edited form as:
Nature. 2013 July 25; 499(7459): 491–495. doi:10.1038/nature12396.

Ptpn11 Deletion in A Novel Cartilage Cell Causes Metachondromatosis by Activating Hedgehog Signaling

Wentian Yang[1,*], **Jianguo Wang**[1], **Douglas C. Moore**[1], **Haipei Liang**[1], **Mark Dooner**[2], **Qian Wu**[3], **Richard Terek**[1], **Qian Chen**[1], **Michael G. Ehrlich**[1], **Peter J. Quesenberry**[2], and **Benjamin G. Neel**[4]

[1]Department of Orthopaedics, Brown University Alpert Medical School and Rhode Island Hospital, Providence, RI 02903

[2]Department of Medicine and COBRE Center for Stem Cell Biology, Rhode Island Hospital and Brown University Alpert Medical School, Providence, RI 02903

[3]Department of Pathology and Laboratory Medicine, University of Connecticut Health Center, Farmington, CT 06030

[4]Princess Margaret Cancer Center, University Health Network, and Department of Medical Biophysics, University of Toronto, Toronto, Ontario, Canada M5G 1L7

Abstract

SHP2, encoded by *PTPN11*, is required for survival, proliferation and differentiation of various cell types[1,2]. Germ line activating mutations in *PTPN11* cause Noonan Syndrome, while somatic *PTPN11* mutations cause childhood myeloproliferative disease and contribute to some solid tumors. Recently, heterozygous inactivating mutations in *PTPN11* were found in metachondromatosis, a rare inherited disorder featuring multiple exostoses, endochondromas, joint destruction and bony deformities[3,4]. The detailed pathogenesis of this disorder has remained unclear. Here, we used a conditional knockout allele (*Ptpn11*^{fl}) and Cre recombinase (Cre) transgenic mice to delete *Ptpn11* specifically in monocytes, macrophages and osteoclasts (lysozyme M-Cre; LysMCre) or in cathepsin K (Ctsk)-expressing cells, previously thought to be osteoclasts. *LysMCre;Ptpn11*$^{fl/fl}$ mice had mild osteopetrosis. Surprisingly, however, *CtskCre;Ptpn11*$^{fl/fl}$ mice developed features strikingly similar to metachondromatosis. Lineage tracing revealed a novel population of Ctsk-Cre-expressing cells in the “Perichondrial Groove of

[*]Corresponding Author: Wentian Yang, M.D., Ph.D., 1 Hoppin Street, Coro 402E, Providence, RI 02903; 401-444-5956 (Phone), wyang@lifespan.org.

Competing interests statement
W.Y. and B.G. N. have filed a provisional patent application on the use of Smoothened inhibitors for the treatment of metachondromatosis (Title: Hedgehog Pathway Inhibition for Cartilage Tumor and Metachondromatosis Treatment; UPA#61/614,449).

Author Contributions W.Y. and B.G.N. conceived the project. J.W., D.M., H.L., and W.Y. carried out most of the experiments. M.D. and W.Y. conducted FACS sorting and analysis. H.L. performed SMOi animal treatment experiment. J.W. performed gene expression and western blot analysis. M.D. and J.W carried out bone marrow transplantation experiments with the advice of P.J.Q.. M.D., H.L and W.Y. performed CPC multi-lineage differentiation assays. Q.W. and R.T. performed histological staining and data interpretation. Q.C. and M.G.E. provided technical and intellectual support. W.Y. and B.G.N. analyzed the data and wrote the manuscript with the help of all authors.

Ranvier" that display markers and functional properties consistent with mesenchymal progenitors. Chondroid neoplasms arose from these cells and showed decreased Erk activation, increased Indian Hedgehog (Ihh) and Parathyroid hormone-related protein (Pthrp) expression and excessive proliferation. Shp2-deficient chondroprogenitors had decreased FGF-evoked Erk activation and enhanced *Ihh* and *Pthrp* expression, whereas FGFR or MEK inhibitor treatment of chondroid cells increased *Ihh* and *Pthrp* expression. Most importantly, Smoothened inhibitor treatment ameliorated metachondromatosis features in *CtskCre;Ptpn11*$^{fl/fl}$ mice. Thus, in contrast to its pro-oncogenic role in hematopoietic and epithelial cells, *Ptpn11* is a tumor suppressor in cartilage, acting via an FGFR/MEK/ERK-dependent pathway in a novel progenitor cell population to prevent excessive *Ihh* production.

Cartilage tumors, including exostoses, enchondromas and chondrosarcomas, comprise ~20% of skeletal neoplasms[5]. Benign and malignant cartilaginous tumors can arise sporadically, but cartilage tumor syndromes, including hereditary multiple exostoses (HME), the multiple enchondromatosis disorders (Ollier disease and Maffucci syndrome), and metachondromatosis (MC), also exist[6,7]. The cellular and molecular pathogenesis of most cartilage tumors is incompletely understood.

MC is an autosomal dominant tumor syndrome featuring multiple exostoses and enchondromas[6,7]. Recently, heterozygous early frameshift or nonsense mutations in *PTPN11* were identified in >50% of MC cases[3,4]. *PTPN11* encodes the non-receptor protein-tyrosine phosphatase SHP2, which is required for RAS/ERK pathway activation in most receptor tyrosine kinase, cytokine receptor, and integrin signaling pathways[1,2]. Germ line activating mutations in *PTPN11* cause Noonan syndrome (NS), whereas mutations that impair SHP2 catalytic activity cause LEOPARD syndrome (LS), both of which can feature skeletal abnormalities[8]. Somatic activating mutations in *PTPN11* are the most common cause of juvenile myelomyelogenous leukemia (JMML) and contribute to other leukemias and some solid tumors[1,2]. Although *PTPN11* is a well-established human oncogene, it is unclear how heterozygous loss-of-function *PTPN11* alleles cause cartilage neoplasms.

Global *Ptpn11* deletion results in early embryonic lethality[9,10], whereas postnatal deletion has context-dependent effects[1,2]. To assess the role of Shp2 in osteoclasts (OC), we crossed *Ptpn11*^{fl} mice[10] to mice expressing Cre under the control of the endogenous lysozyme M (LysM)[11] or cathepsin K[12] (Ctsk) promoter. The LysM promoter is active in monocytes, macrophages and osteoclast precursors[11], whereas the Ctsk promoter reportedly is active only in mature OC[12,13]. These crosses generated *Ptpn11*$^{fl/+}$*;LysMCre* and *Ptpn11*$^{fl/fl}$*;LysMCre* (hereafter, LysM-Control and LysM-KO) and *Ptpn11*$^{fl/+}$*;CtskCre* and *Ptpn11*$^{fl/fl}$*;CtskCre* (hereafter, Ctsk-Control and Ctsk-KO) mice, respectively (Fig. 1a).

Neither *Ptpn11*$^{fl/+}$*;LysMCre*, nor *Ptpn11*$^{fl/+}$*;CtskCre*, mice had a discernible phenotype, so we focused all subsequent analyses on LysM-KO and Ctsk-KO mice. Shp2 levels were reduced by >80% in bone marrow-derived macrophages (BMM) and OC in LysM-KO and Ctsk-KO mice (Fig. S1a **and data not shown)**. LysM-KO and Ctsk-KO mice were born at the expected Mendelian ratios and appeared normal for their first 3 weeks post-birth. Subsequently, LysM-KO mice developed mild, age-related osteopetrosis (Fig. S1b **and data**

not shown). By contrast, within eight weeks after birth, Ctsk-KO mice exhibited a dramatic skeletal phenotype, comprising decreased body length, increased bone mineral density, scoliosis, metaphyseal exostoses and markedly decreased mobility (Fig. 1b–d & Supplementary video clips 1,2). Sections of hind limb paw and knee joints from 12-week-old Ctsk-KO mice revealed multiple exostoses and enchondromas at the metaphyses of their metatarsals and phalanges (Fig. 1d), tibiae and femurs (Fig. S1c,d), and other bones **(data not shown)**, features reminiscent of MC. As heterozygous *PTPN11* frameshift mutations cause MC[3,4], these findings indicate that *PTPN11* is a cartilage tumor suppressor gene, and suggest that loss (or silencing) of the remaining *PTPN11* allele is required for tumor formation.

To identify the cells responsible for MC-like disease in Ctsk-KO mice, we first injected bone marrow (BM) from 6-week-old Ctsk-KO and Ctsk-Control mice (C57/BL6; CD45.2) into lethally irradiated 3-week-old recipients (B6.SJL; CD45.1). Recipient mice exhibited high chimerism (Fig. S2a,b), but did not develop cartilage tumors in over 12 months of observation. Consistent with the osteopetrosis seen in LysM-KO mice, recipients had increased bone mineral density (Fig. S2c). Clearly, though, cartilage tumors in Ctsk-KO mice are not due to altered OC development/function.

Next, we performed lineage-tracing studies, using *Rosa26LSL-lacZ* (*R26LSL-lacZ*) or *Rosa26LSL-YFP* (*R26LSL-YFP*) Cre reporter mice. Remarkably, CtskCre, but not LysMCre, was expressed in a subset of perichondrial cells within the so-called “Groove of Ranvier” (Fig. 2a). Sections from knee joints collected at P10 revealed significant expansion of a cluster of Alcian blue/Safranin O-positive cells in this region in Ctsk-KO, mice, but not in Controls (Fig. 2b, **boxed region and** Fig. S1c). By post-natal week 2, the YFP^+ cell population had expanded and differentiated into ectopic cartilaginous tissue in compound Ctsk-KO/YFP reporter mice (Fig. 2c, **boxed region**). Exostoses were palpable at 6 weeks and visible by 8–12 weeks. In compound Ctsk-KO/YFP reporter mice, these lesions consisted of YFP^+ chondroid cells at various stages of development, including proliferating, pre-hypertrophic, and hypertrophic chondrocytes, as revealed by cell morphology and Col2α1 and Col10α1 immunostaining (Fig. 2c,d **and data not shown**). Notably, nearly all chondroid tumor cells were YFP^+ (Fig. 2c **and** S2d). Hence, cartilaginous tumors in Ctsk-KO mice (and, by analogy, most likely in MC) result from cell-autonomous lack of Shp2 in Ctsk+ cells from the Perichondrial Groove of Ranvier.

The Perichondrial Groove of Ranvier is believed to contain chondroprogenitors responsible for circumferential cartilage growth, but these cells are not well-characterized[14,15]. We used flow cytometry to analyze epiphyseal cartilage cells harvested from the distal femurs and proximal tibiae of Ctsk-Control/YFP and Ctsk-KO/YFP mice at P10–12. Compared with controls, the frequency of YFP^+ cartilage cells in Ctsk-KO/YFP mice was increased by ~5-fold (Fig. 3a). Within the YFP^+ cell population, the percentage of cells expressing CD44, CD90, and CD166 (mesenchymal progenitor markers), but not CD31 (endothelial cell marker), also was increased (Fig. 3b). Staining for Stro1 and Jagged1, markers associated with presumptive chondroprogenitors in the groove based on BrdU label retention studies[16], was more intense in Ctsk-KO mice (Fig. 3c). Moreover, YFP^+ cells were capable of multi-lineage differentiation *in vitro*, as assessed by Alcian Blue, Oil Red O and Alizarin red

staining, respectively (Fig. 3d). These data suggest that Shp2 regulates the proliferation of a novel cartilage cell population characterized by Ctsk expression, which we hereafter term "Ctsk+ Chondroid Progenitors" (CCPs).

Multiple pathways control cartilage development and homeostasis[17]. Indian hedgehog (IHH) and Parathyroid hormone-related protein (PTHRP) signaling are particularly important, and aberrant regulation of these pathways causes developmental defects and skeletal tumors[18,19]. We examined chondrogenic gene expression in cartilage tumors from Ctsk-KO mice by quantitative reverse-transcription PCR (qRT-PCR). Consistent with our immunostaining data (Fig. 2d), *Col2α1 and Col10α1* transcripts were increased. Furthermore, *Ihh* and *Pthrp* levels were elevated substantially (Fig. 4a, S3a).

These findings prompted us to ask whether Shp2 regulates *Ihh* and *Pthrp* production, and if so, how. During development, cells within the perichondrium make Fgf18, which can signal to adjacent cells via Fgfr3 to suppress *Ihh* expression[20,21]. As Shp2 is required for Fgfr signaling in other cell types[1,2], we suspected that Shp2 might be required for Fgfr3-induced suppression of *Ihh* expression. We therefore examined the status of Fgfr3 signaling components and *Ihh* expression in CCPs. Erk activation, as assayed by Tyr204Thr202 phosphorylation, was compromised in the absence of Shp2, whereas Akt (p-Ser473) and Stat1/3 (p-Tyr807) activation were unaffected (Fig. 4a, S3b **& data not shown**). Furthermore, consistent with our qRT-PCR data, *Ihh* mRNA and protein were elevated in Shp2-deficient CCPs (Fig. 4a). Ihh antibody specificity was confirmed by immunostaining of growth plate cartilage (Fig. S3c).

CCPs are rare, rendering their detailed biochemical analysis unfeasible. We therefore tested the effects of Shp2 depletion in ATDC5 chondroid cells by stably expressing either of two shRNAs targeting mouse *Ptpn11*. As in Ctsk-KO mice (Fig. 4a), Fgf18-evoked Erk activation was decreased, while *Ihh* and *Pthrp* levels were increased in Shp2-deficient cells (Fig. 4b). Conversely, FGFR (PD173074) or MEK (UO126) inhibition led to enhanced *Ihh* and *Pthrp* expression in parental ATDC5 cells (Fig. 4c).

Ihh signaling evokes Pthrp production[22]. Our data, and previous studies[23], suggested that increased Ihh levels might be pathogenic in MC. If so, then blocking or attenuating Ihh signaling might slow and/or prevent the disease. To test this hypothesis, Control (wild type) and Ctsk-KO mice (9/group) were gavaged daily with the Smoothened inhibitor PF-04449913 (SMOi, 100μg/g body weight) or vehicle control (0.5% methylcellulose), beginning at 5 weeks of age (when early lesions were present) and continuing for the succeeding 4 weeks. Skeletal phenotype was assessed by X-ray, μ-CT, and histology. Remarkably, SMOi treatment significantly reduced the number of exostoses in Ctsk-KO mice (Fig. 4d, S4–7), and dramatically improved their mobility (Supplemental Video clips 1,2), without apparent effects on overall growth rate (Fig. S8). Importantly, SMOi levels in treated mice were adequate to suppress Ihh target gene expression in exostoses (Fig. S7b).

Our findings strongly suggest that MC results from loss of SHP2 specifically in CCPs, a heretofore poorly characterized population within the Perichondrial Groove of Ranvier, which is believed to function as a stem cell niche for joints[16] and a reservoir for the

germinal layer cells of the growth plate[24]. Cells within the Groove of Ranvier express high levels of FGFR3[25], and their removal prevents longitudinal bone growth[26]. Emerging evidence shows that Groove of Ranvier cells can migrate into articular cartilage[16], implicating them in maintaining cartilage homeostasis and possibly in degenerative joint diseases, such as osteoarthritis. Indeed, in lineage tracing studies of normal mice, we noticed YFP^+ cells migrating towards articular cartilage (Fig. S9, **arrows, and data not shown)**. Based on our mouse MC model, we propose that SHP2, acting downstream of FGFR3 and upstream of the RAS/ERK pathway, regulates CCP proliferation and chondrogenic differentiation. Consequently, *PTPN11* deficiency in these cells promotes excessive proliferation, chondrogenic differentiation, and cartilage tumors.

MC is associated with heterozygous inactivating mutations in *PTPN11*, yet *Ptpn11$^{fl/+}$;CtskCre* mice are normal, whereas Ctsk-KO mice exhibit MC-like features. Although *PTPN11* gene dosage effects could differ in mouse and man (and thus 50% reduction in SHP2 level might cause MC in humans but not in mice), we think it is more likely that loss of the remaining *PTPN11* allele (e.g., by LOH or silencing) is required to cause cartilage tumors in MC. If so, then unlike its oncogenic role in JMML, other hematologic malignancies and solid tumors[1,2], *PTPN11* is a tumor suppressor in cartilage. Liver-specific *Ptpn11* deletion reportedly results in hepatocellular carcinoma[27]. However, we have not seen liver tumors in our *Ptpn11* conditional knockout mice crossed to the same Cre line (F. H. and B.G.N., manuscript in preparation), nor is *PTPN11* mutated in human hepatocellular carcinoma. Moreover, our biochemical and pharmacological analysis, together with previous studies, provide a parsimonious and attractive explanation for the apparently paradoxical pro- and anti-oncogenic effects of *PTPN11*. In both cases, SHP2 is a critical regulator of ERK. The activating *PTPN11* mutations associated with cancer promote proliferation and survival, at least in part via increased ERK activation. Similarly, over-expression or increased activation of normal SHP2 binding proteins such as GAB2, or the presence of pathologic SHP2 binding proteins such as *H. pylori* CagA[28], can hyperactivate ERK and contribute to various malignancies. Conversely, SHP2 deficiency is oncogenic in CCPs because in these cells, ERK normally represses the expression of the growth stimulator IHH (which in turn, stimulates PTHRP production). Future studies should focus on better defining the properties of CCPs, determining whether *PTPN11* also acts as a tumor suppressor in other cartilage neoplasms, including chondrosarcoma, and most importantly, on testing the effects of Smoothened inhibition in MC patients. Finally, given our proposed mechanism of MC pathogenesis, our results argue for caution in the long term use of MEK or ERK inhibitors.

Methods

Antibodies and Reagents

The following antibodies were purchased: monoclonal anti-phospho(p)-tyrosine (4G10) was from Millipore; polyclonal antibodies against phospho(p)-Erk1/2, Erk2, p-Akt(Ser473), Akt, Shp2, p-Stat1(Tyr701) and Stat1 were from Cell Signaling; antibodies against Ihh, Col2α1, and Col10α1 were from Santa Cruz Biotechnology and Abcam, respectively; fluorescence-labeled antibodies against CD31, CD44, CD45, CD90, and CD166 were purchased from

eBioscience; and antibodies against Stro1 and Jagged1 were purchased from Invitrogen and Epitomics, respectively. Alexa488-labeled goat anti-rabbit IgG and Alexa594-labeled anti-rabbit and anti-mouse IgG were purchased from Invitrogen. FGF18 was purchased from Peprotech. UO126 and PD173074 were from Calbiochem and Selleckbio, respectively. PF-04449913 was kindly provided by Pfizer, Inc. Alcian blue, Alizarin red S, and Oil red O staining solutions were purchased from Poly Scientific.

Cell isolation and culture

To isolate YFP^+ cartilage cells (CCPs), epiphyseal cartilage was dissected from 2-week-old Ctsk-Control/YFP and Ctsk-KO/YFP mice, and digested with hyaluronidase (2.5 mg/ml, Sigma) and Trypsin-EDTA (0.25%, Invitrogen) to remove soft tissues, and then with collagenase D (2.5 mg/ml, Roche) for 4–6 hours to release all cartilage cells. After washing in PBS, cells were stained with fluorescence-labeled antibodies (using concentrations recommended by the manufacturers), and analyzed by flow cytometry, or YFP^+ cells were purified by FACS and placed in short-term cultures (3–4 days) in murine mesenchymal culture medium (StemCell Technologies) containing 10% FBS.

Parental ATDC5 cells were obtained from Dr. Chanika Phornphutkul (Brown University) and cultured in complete DMEM/F12 medium (1:1) (Invitrogen), as described[31]. Short hairpin RNAs against mouse *Ptpn11* (kd1: 5′-GATTCAGAACACTGGGGACTTCAAGAGAGTCCCCAGTGTTC TGAATC; kd2: 5′-GAGTAACCCTGGAGACTTCTTCAAGAGAGAAGTCTCCAGGGTTA CTC), or a scrambled control for kd1 (5′-TAGTACAAGTCCAAGCGGCTTCAAGAGAGCCGCTGGACTTGTACTA), were introduced into the retroviral vector **pSuper**(retro)/puro (Oligoengine). Viral supernatants were collected from 293T cells co-transfected with each retroviral vector and Ecopac, and used to infect ATDC5 cells, which were then selected with puromycin[32].

Differentiation assays

CCPs (~ 2×10^4), purified by FACS (for YFP) from 10–14 day old *Ctsk-R26LSL-YFP* reporter mice, were cultured in differentiation medium for chondrocytes (DMEM with 10% FBS, 0.1μM Dexamethasone, 0.1mM Ascorbic acid, 10mM Glycerol 2-phosphate, TGFβ1 1ng/ml), adipocytes (DMEM with 10% FBS, 1μM Dexamethasone, 0.5mM IBMX, 10ug/ml Insulin), or osteoblasts (DMEM with 10% FBS, 0.1μM Dexamethasone, 0.2mM Ascorbic acid, 10mM Glycerol2-phosphate, 10ng/ml rhMBP2), respectively. After culturing for 2 (adipogenic or chondrogenic differentiation) or 3 weeks (osteogenesis) cells were fixed and stained with Alcian blue, Oil red O or Alizarin red to visualize the formation of cartilage, fate, and bone tissue, respectively.

Quantitative RT-PCR

RNA was extracted from cultured cells or cartilage lesions enriched by laser-capture using the RNeasy kit (Qiagen). cDNA was synthesized using iScript™cDNA Synthesis Kit (Bio-Rad), and qRT-PCR was performed by using the iQ™SYBR®Green qPCR kit. All values were normalized to *Gapdh* levels, and qRT-PCR data were expressed as fold-increases

compared with controls. Primer sequences and PCR conditions are available from W.Y. upon request.

Flow Cytometry and FACS

Epiphyseal cartilage cells were stained with fluorescence-labeled antibodies, as described,[33] and analyzed on a BD™ LSR II flow cytometer. YFP^+ cells were purified by FACS using a BD Influx™ cell sorter (BD Bioscience, San Diego, CA). Flow cytometric data were analyzed with FlowJo software (TreeStar).

Histology

Ctsk-Control and -KO mice were euthanized at the indicated ages, and femurs, tibiae, and paws were removed and fixed in 4% PFA overnight at 4°C. Postnatal skeletal tissues were decalcified in 0.5M EDTA before embedding. Tissue sections (5μm) were stained with H&E, Alcian blue, or Safranin O. Immunofluorescence staining was carried out using secondary antibodies conjugated to the indicated fluorophores at concentrations recommended by their manufacturers. Immunohistochemistry was performed using fluorescence- or peroxidase-coupled anti-rabbit, mouse, or -goat secondary antibodies, as per the manufacturer's instructions, with DAB serving as the substrate. X-gal staining was performed as described[12].

Drug Treatment

Two trials were performed using the Smoothened inhibitor PF-04449913. In a pilot study, groups (5 mice/each) of KO mice were treated with SMOi (100μg/g body weight) or vehicle control (0.5% methylcellulose), beginning at 5 weeks of age (at which time early lesions were present) and continuing for the succeeding 4 weeks. Mice were randomized by alternate assignment to control (vehicle) or drug treatment arms. The pilot experiment showed a significant difference in number of exostoses (assessed radiographically) in the SMOi group, and led to a second study (again involving 5 mice each) to confirm these findings and also assess additional parameters (μCT, histology, gene expression). Two mice (one each from control and experimental groups, respectively) died for unknown reasons during the second trial, and were excluded from the analysis because they were removed from cages and could not be recovered. All surviving mice from both studies were included in the analyses shown in the text.

Microcomputed Tomography (μ-CT) and X-Ray Analysis

X-ray images of the entire skeleton, knees, metatarsals and phalanges were obtained immediately after euthanasia by using a Faxitron X-ray system (Wheeling, Illinois). After fixation in 4% PFA, μ-CT images of skeletal tissues were scanned with a desktop microcomputer graphic imaging system (μ-CT40, Scanco Medical AG, CH). The number of exostoses was measured from these radiographic images, as indicated in the Figure legends. For these studies, mice were assigned a code number by the animal technician, and blinded quantification was carried out by W.Y.

Immunoblotting

Cells were lysed in NP-40 buffer (0.5% NP40, 150 mM NaCl, 1 mM EDTA, 50 mM Tris [pH 7.4]), supplemented with a protease inhibitor cocktail (1 mM PMSF, 1 mM NaF, 1 mM sodium orthovanadate, 10 mg/ml aprotinin, 0.5 mg/ml antipain, and 0.5 mg/ml pepstatin), as described[10]. For immunoblotting, cell lysates (10–50 μg) were resolved by SDS-PAGE, transferred to PVDF membranes, and incubated with primary antibodies for 2 hr or overnight at 4°C (according to the manufacturer's instructions), followed by HRP-conjugated secondary antibodies. Detection was by enhanced chemiluminescence (Amersham). Signals were quantified using NIH ImageJ.

Statistical Analysis

Differences between groups were evaluated by Student's *t* test. A p value of <0.05 was considered significant. For all of these experiments, between groups variances were similar and data were symmetrically distributed. All analyses were performed by using Excel (Microsoft, Redmond, WA) and Prism 3.0 (GraphPad, San Diego, CA).

Supplementary Material

Refer to Web version on PubMed Central for supplementary material.

Acknowledgments

We thank Dr. Shigeaki Kato (University of Tokyo) for Ctsk-Cre mice, Dr. April Craft (Princess Margaret Cancer Center) for review of the manuscript, Ms. Xiaohong Wang and Mr. Paul Monfils for help with histology, and Dr. Jay Cao (USDA) for helping μ-CT analysis. This publication was made possible by NIH and the National Institute for General Medicine Sciences (NIGMS) Grant #8P20GM103468. This work was also funded by NIH R21AR57156 (to W.Y) and R37CA49152 (to B.G.N.), the Rhode Island Hospital Orthopaedic Foundation and a grant from the Pediatric Orthopaedic Society of North America and the Orthopaedic Research and Education Foundation (to W.Y.). B.G.N. is a Canada Research Chair, Tier 1, and also is supported in part by the Ontario Ministry of Health and Long Term Care and the Princess Margaret Cancer Foundation.

References

1. Neel BG, Chan G, Dhanji S. SH2 Domain-Containing Protein-Tyrosine Phosphatases. Handbook of Cell Signaling. 2009:771–809.
2. Grossmann KS, Rosario M, Birchmeier C, Birchmeier W. The tyrosine phosphatase Shp2 in development and cancer. Adv Cancer Res. 2010; 106:53–89. [PubMed: 20399956]
3. Bowen ME, et al. Loss-of-function mutations in PTPN11 cause metachondromatosis, but not Ollier disease or Maffucci syndrome. PLoS Genet. 2011; 7:e1002050. [PubMed: 21533187]
4. Sobreira NL, et al. Whole-genome sequencing of a single proband together with linkage analysis identifies a Mendelian disease gene. PLoS Genet. 2010; 6:e1000991. [PubMed: 20577567]
5. Bovee JV, Hogendoorn PC, Wunder JS, Alman BA. Cartilage tumours and bone development: molecular pathology and possible therapeutic targets. Nat Rev Cancer. 2010; 10:481–488. [PubMed: 20535132]
6. Pannier S, Legeai-Mallet L. Hereditary multiple exostoses and enchondromatosis. Best Pract Res Clin Rheumatol. 2008; 22:45–54. [PubMed: 18328980]
7. Pansuriya TC, Kroon HM, Bovee JV. Enchondromatosis: insights on the different subtypes. Int J Clin Exp Pathol. 2010; 3:557–569. [PubMed: 20661403]
8. Tartaglia M, Gelb BD, Zenker M. Noonan syndrome and clinically related disorders. Best practice & research. Clinical endocrinology & metabolism. 2011; 25:161–179. [PubMed: 21396583]

9. Saxton T, et al. Abnormal mesoderm patterning in mouse embryos mutant for the SH2 tyrosine phosphatase Shp-2. EMBO J. 1997; 16:2352–2364. [PubMed: 9171349]
10. Yang W, et al. An Shp2/SFK/Ras/Erk signaling pathway controls trophoblast stem cell survival. Dev Cell. 2006; 10:317–327. [PubMed: 16516835]
11. Clausen BE, Burkhardt C, Reith W, Renkawitz R, Forster I. Conditional gene targeting in macrophages and granulocytes using LysMcre mice. Transgenic Res. 1999; 8:265–277. [PubMed: 10621974]
12. Nakamura T, et al. Estrogen prevents bone loss via estrogen receptor alpha and induction of Fas ligand in osteoclasts. Cell. 2007; 130:811–823. [PubMed: 17803905]
13. Dodds RA, Connor JR, Drake F, Feild J, Gowen M. Cathepsin K mRNA detection is restricted to osteoclasts during fetal mouse development. J Bone Miner Res. 1998; 13:673–682. [PubMed: 9556067]
14. Langenskiold A. Role of the ossification groove of Ranvier in normal and pathologic bone growth: a review. J Pediatr Orthop. 1998; 18:173–177. [PubMed: 9531398]
15. Shapiro F, Holtrop ME, Glimcher MJ. Organization and cellular biology of the perichondrial ossification groove of ranvier: a morphological study in rabbits. J Bone Joint Surg Am. 1977; 59:703–723. [PubMed: 71299]
16. Karlsson C, Thornemo M, Henriksson HB, Lindahl A. Identification of a stem cell niche in the zone of Ranvier within the knee joint. J Anat. 2009; 215:355–363. [PubMed: 19563472]
17. Goldring MB, Tsuchimochi K, Ijiri K. The control of chondrogenesis. J Cell Biochem. 2006; 97:33–44. [PubMed: 16215986]
18. Hopyan S, et al. A mutant PTH/PTHrP type I receptor in enchondromatosis. Nat Genet. 2002; 30:306–310. [PubMed: 11850620]
19. Tiet TD, et al. Constitutive hedgehog signaling in chondrosarcoma up-regulates tumor cell proliferation. The American journal of pathology. 2006; 168:321–330. [PubMed: 16400033]
20. Liu Z, Xu J, Colvin JS, Ornitz DM. Coordination of chondrogenesis and osteogenesis by fibroblast growth factor 18. Genes Dev. 2002; 16:859–869. [PubMed: 11937493]
21. Ohbayashi N, et al. FGF18 is required for normal cell proliferation and differentiation during osteogenesis and chondrogenesis. Genes Dev. 2002; 16:870–879. [PubMed: 11937494]
22. Kronenberg HM. PTHrP and skeletal development. Ann N Y Acad Sci. 2006; 1068:1–13. [PubMed: 16831900]
23. Murakami S, et al. Constitutive activation of MEK1 in chondrocytes causes Stat1-independent achondroplasia-like dwarfism and rescues the Fgfr3-deficient mouse phenotype. Genes Dev. 2004; 18:290–305. [PubMed: 14871928]
24. Fenichel I, Evron Z, Nevo Z. The perichondrial ring as a reservoir for precartilaginous cells. In vivo model in young chicks' epiphysis. Int Orthop. 2006; 30:353–356. [PubMed: 16652202]
25. Robinson D, et al. Fibroblast growth factor receptor-3 as a marker for precartilaginous stem cells. Clin Orthop Relat Res. 1999:S163–175. [PubMed: 10546645]
26. Rodriguez JI, Delgado E, Paniagua R. Changes in young rat radius following excision of the perichondrial ring. Calcified tissue international. 1985; 37:677–683. [PubMed: 3937595]
27. Bard-Chapeau EA, et al. Ptpn11/Shp2 acts as a tumor suppressor in hepatocellular carcinogenesis. Cancer cell. 2011; 19:629–639. [PubMed: 21575863]
28. Hatakeyama M. Oncogenic mechanisms of the Helicobacter pylori CagA protein. Nat Rev Cancer. 2004; 4:688–694. [PubMed: 15343275]
29. Soriano P. Generalized lacZ expression with the ROSA26 Cre reporter strain. Nat Genet. 1999; 21:70–71. [PubMed: 9916792]
30. Srinivas S, et al. Cre reporter strains produced by targeted insertion of EYFP and ECFP into the ROSA26 locus. BMC Dev Biol. 2001; 1:4. [PubMed: 11299042]
31. Hidaka K, et al. Involvement of the phosphoinositide 3-kinase/protein kinase B signaling pathway in insulin/IGF-I-induced chondrogenesis of the mouse embryonal carcinoma-derived cell line ATDC5. The international journal of biochemistry & cell biology. 2001; 33:1094–1103. [PubMed: 11551825]

32. Mohi MG, et al. Prognostic, therapeutic, and mechanistic implications of a mouse model of leukemia evoked by Shp2 (PTPN11) mutations. Cancer cell. 2005; 7:179–191. [PubMed: 15710330]

33. Pretzel D, et al. Relative percentage and zonal distribution of mesenchymal progenitor cells in human osteoarthritic and normal cartilage. Arthritis research & therapy. 2011; 13:R64. [PubMed: 21496249]

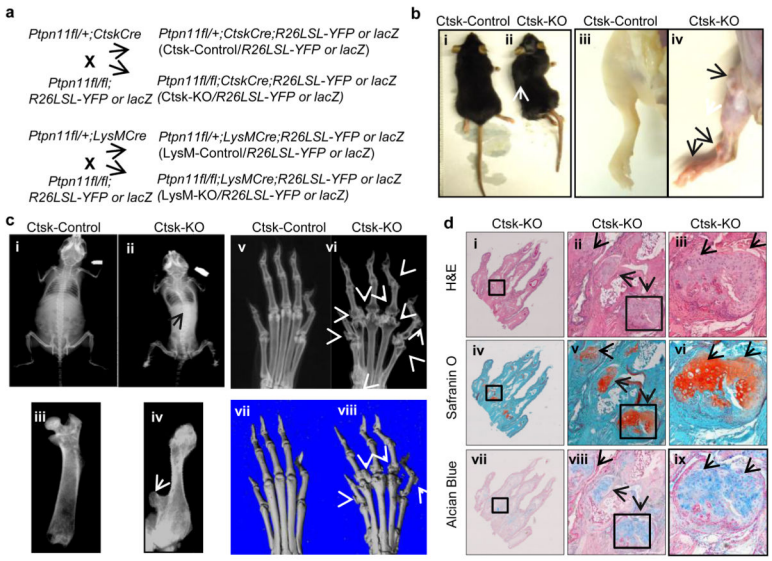

Figure 1.

Ptpn11 deletion in Cathepsin K-expressing cells causes metachondromatosis. **a,** Schemes for generating Ctsk-KO, LysM-KO, and Control mice. Gross images (**b**) and Faxitron/μ-CT radiographs (**c**) of 12 week-old Ctsk-KO mice showing dwarfism and scoliosis (**b.ii**, white arrow; **c.ii**, black arrow), increased bone mineral density (**c.ii,iv**) and multiple exostoses of knees, ankles, and metatarsals (**b.iv; c.ii,iv,vi,viii**; arrowheads) with joint destruction. **d,** Sagittal sections of metatarsal joints stained with H&E (**i–iii**), Safranin O (**iv–vi**) and Alcian blue (**vii–ix**) showing cartilaginous exostoses and enchondromas (arrows) in Ctsk-KO mice. Images in **iii, vi** and **ix** are magnified (10X) views of boxed areas in **ii, iv** and **viii,** respectively. Data shown are representative images; each analysis was performed on at least 5 mice/genotype.

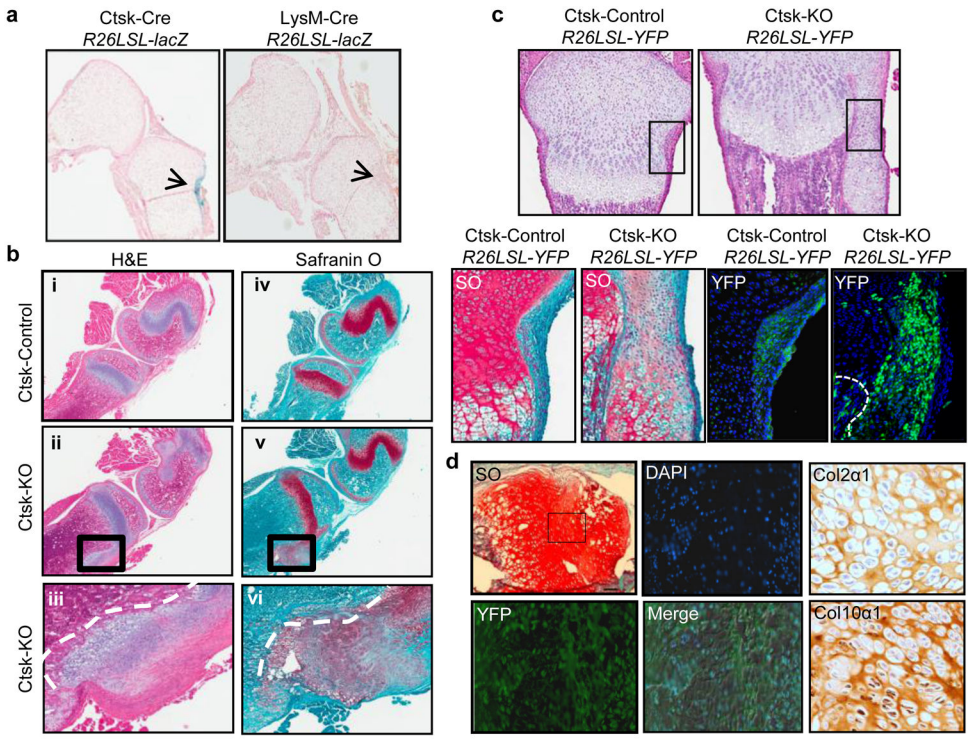

Figure 2.

Skeletal tumors in Ctsk-KO mice originate from Perichondrial Groove of Ranvier cells. **a**, X-gal staining of knee joint sections from 1-week-old *R26LSLlacZ;Ctsk-Cre* and *R26LSLlacZ;LysM-Cre* reporter mice showing that the Ctsk (but not the LysM) promoter is active not only in osteoclasts, but also in a subset of cells from the Perichondrial Groove of Ranvier (arrows). **b**, H&E and Safranin O staining of knee joint sections from P10 Ctsk-Control (**i,iv**) and Ctsk-KO (**ii,iii,v,vi**) mice showing expansion of cells within the Perichondrial Groove of Ranvier region in Ctsk-KO mice. Images in **iii & vi** are magnified (10x) views of boxed areas in **ii & v** respectively; **c,** H&E-and Safranin O-stained sections showing expanding YFP^+ population within the Perichondrial Groove of Ranvier (boxed region in top panels, magnified below) that also stains with Safranin O, indicative of cartilage. Dashed line marks boundary between marrow/growth plate and perichondrial groove. **d**, frozen section of an exostosis from the metatarsal joint of Ctsk-KO/YFP mice showing co-localization of YFP reporter with cartilaginous tumor cells (boxed area). Note that the lesion is enriched in proliferating and pre-hypertrophic chondrocytes, as shown by overlapping Col2α1 and Col10α1 immunostaining. Each panel is a representative image from one mouse; each analysis was performed on at least 3 mice/genotype.

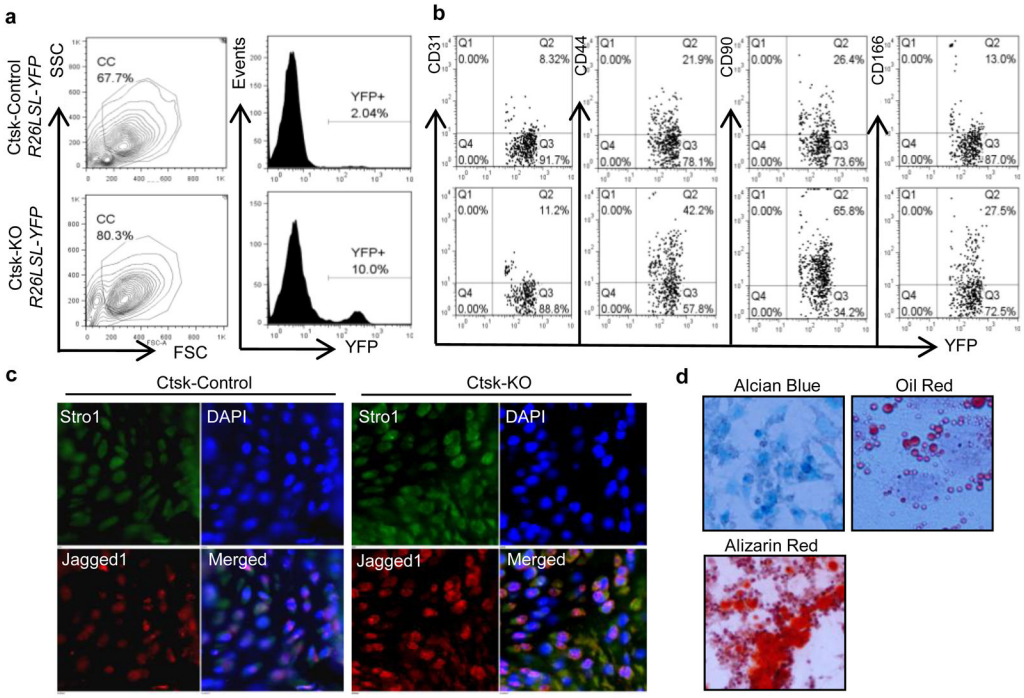

Figure 3.

Ptpn11 deletion in Ctsk-expressing cells causes expansion of novel chondroprogenitor cell population within the Perichondrial Groove of Ranvier. **a,** Flow cytometric analysis showing YFP^+ cells from pooled epiphyseal cartilage from 5–7 Ctsk-Control/YFP mice; note increased percentage of such cells in 2-week-old Ctsk-KO/YFP mice. CC: Chondroid cells. **b,** Flow cytometric analysis of YFP^+ perichondrial cells showing staining for CD31, CD44, CD90, and CD166. Data in panels **a** and **b** are from a single experiment; similar results were obtained in 2 additional experiments. **c,** Immunofluorescence micrograph showing Stro1 and Jagged1 expression in YFP^+ perichondrial cells. Nuclei are stained with DAPI. Note enhanced intensity of Stro1 and Jagged staining in Ctsk-KO cells. Data shown are from single mice of each genotype; two additional mice were analyzed for each genotype with similar results. **d,** CCPs give rise to cartilage, fat and bone. FACS-purified YFP^+ cells from 5–7 mice were subjected to differentiation assays in triplicate. After 2–3 weeks of culture (see Methods), cells were fixed and stained with Alcian blue, Oil red, and Alizarin red to visualize the formation of cartilage, fat, and bone tissue, respectively.

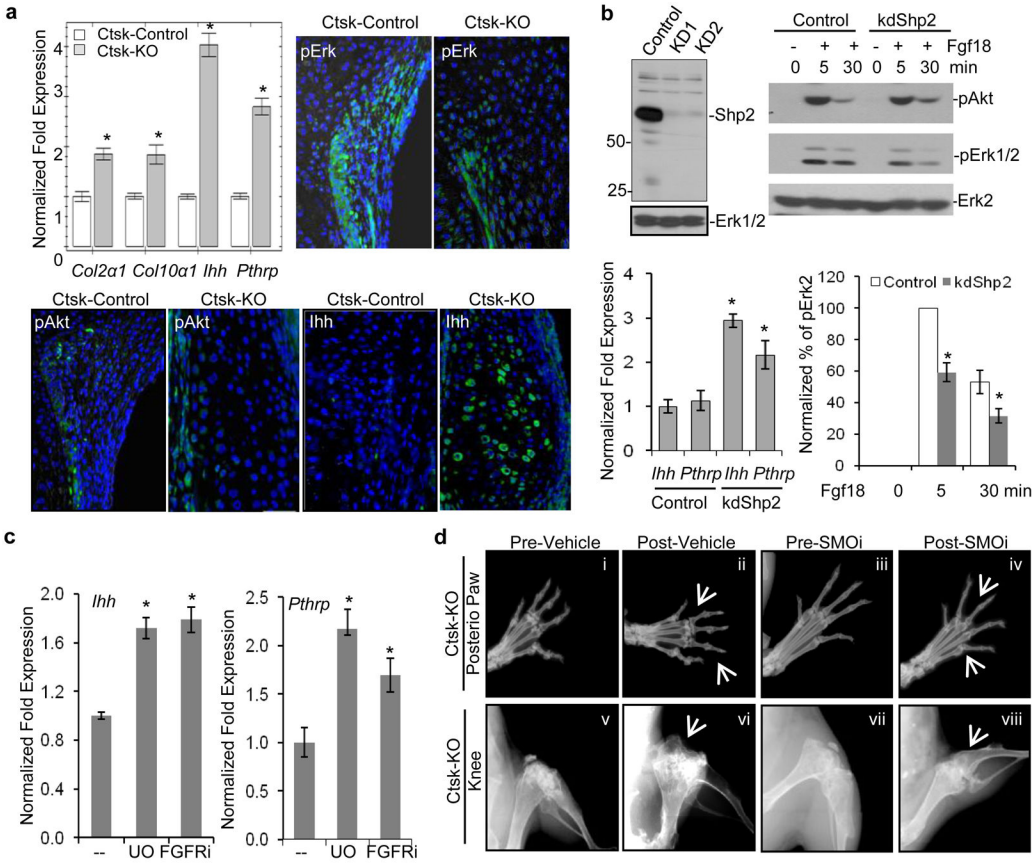

Figure 4.

Shp2 deficiency impairs Erk activation but promotes *Ihh* and *Pthrp* expression. **a,** (Left panel) qRT-PCR showing increased *Col2α1*, *Col10α1*, *Ihh*, and *Pthrp* expression in laser-captured cartilaginous cells from exostoses in 4 mice/genotype, compared with normal articular cartilage cells (mean±S.D; **p*<0.05, 2-tailed Student's *t* test). (Right panel) Immunostaining of representative paraffin sections from Perichondrial Groove of Ranvier region of Ctsk-KO and Control mice. Note the decreased number of p-Erk+ cells (75.4% in Ctsk-Control vs 32.2% in Ctsk-KO; n=3 mice), but increased Ihh expression in Ctsk-KO, compared with Control, mice. **b,** (Left Panel) Immunoblot showing Shp2 in ATDC5 cells stably expressing shRNAs against mouse *Ptpn11* (ATDC5-KD1, ATDC5-KD2, respectively) or scrambled control hairpin. (Right panels). Representative blot showing that Shp2 deficiency decreases Erk activation in response to Fgf18 (top); data from multiple experiments (n=3) showing pErk levels (compared with control at 5 minutes, mean±S.D.; *p*<0.05, 2-tailed Student's *t* test) are quantified below. qRT-PCR (bottom left) shows increased *Ihh* and *Pthrp* expression in Shp2-deficient ATDC5 cells (mean ± S.D.; n=3, **p*<0.05, 2-tailed Student's *t* test). **c,** FGFR (PD173074, 10nM) or MEK (UO126, 1μM) inhibitor treatment of parental ATDC5 cells enhances *Ihh* and *Pthrp* expression, as shown by qRT-PCR (mean±S.D; n=3, **p*<0.05, 2-tailed Student's *t* test). **d,** Faxitron radiographs showing that Hedgehog pathway blockade following administration of the Smoothened inhibitor PF-04449913 (100μg/g body weight) to Ctsk-KO mice ameliorates tumor formation, compared with vehicle control (0.5% methylcellulose)-treated mice. Images of

representative posterior paws **(i–iv)** and knees (**v–vii)** taken pre- **(i,iii,v,vii)** and post-treatment with Vehicle **(ii,vi)** or Smoothened inhibitor (SMOi) **(iv,viii)** for 4 weeks. Note continued development of exostoses and endochromas in Vehicle-treated mice, and their amelioration in SMOi-treated group (arrows). Also, see Figs. S4–S7 and Supplemental video clips 1,2.